Available online at www.sciencedirect.com

ScienceDirect

IFAC PapersOnline CONFERENCE PAPER ARCHIVE

IFAC PapersOnLine 51-29 (2018) 360–365

Semantic SLAM for an AUV using object recognition from point clouds

K. Himri * **P. Ridao** * **N. Gracias** * **A. Palomer** *
N. Palomeras * **R. Pi** *

* *Computer Vision and Robotics Institute, Universitat de Girona, Pic de Peguera 13, 17003 Girona, Spain (e-mail: author@udg.edu).*

Abstract: This paper presents a navigation and mapping system for an autonomous underwater vehicle (AUV) while operating near a man-made underwater environment. The objective is to recognize objects (or object parts) and use these as landmarks for simultaneous localization and mapping (SLAM). This approach is intended as the first step towards autonomous object manipulation, to be carried out at a later stage. The approach contains two main components: Object recognition from range data, and feature-based semantic SLAM. For the first component we propose an automatic method for the recognition and location of 3D objects using 3D point clouds as input, extracted from a laser scanner. Since it is common in inspection maintenance and repair (IMR) applications to have access to the 3D models of the objects of interest, the proposed method assumes *a priori* knowledge of the 3D models of these objects. In typical man-made environments, such objects can be distinct components of a structure, such as valves, pipes and wet-mateable connectors. The object recognition is based on recently proposed *global descriptors* for point clouds, that allow a compact description of the object shape, which is independent of the object view point. Once an object is recognized, its pose with respect to the AUV is determined using an ICP-based method. The second component of the approach is a feature based SLAM algorithm that uses the recognized objects as landmarks to improve the AUV navigation. The paper presents preliminary results obtained with the Girona 500 AUV, equipped with a fast laser scanner recently developed at the University of Girona. Tests conducted in a controlled environment (water tank) illustrate the suitability of the approach.

Keywords: 3D object recognition, 3D global descriptor, simultaneous localization and mapping (SLAM), Viewpoint Features Histogram (VFH), Ensemble of Shape Functions (ESF), laser scanner, autonomous underwater vehicles (AUVs).

1. INTRODUCTION

Nowadays, intervention operations for inspection maintenance and repair (IMR) are carried out using work class ROVs. Commonly, to conduct IMP operations, two pilots cooperate: one being in charge of guiding the ROV while the other one controls the robot arm. During the last years, the research community working in mobile robots and humanoids equipped with arms, operating in structured environments, started to pave the way towards advanced manipulation systems able to explore the environment and discover 3D objects to be manipulated. There has been significant progress, for instance using robots in kitchen environments like Rusu et al. (2008c,a); Blodow et al. (2011), where robots were able to identify everyday objects (such as a bowl, a place, or a glass) using RGB-D cameras, as well as to locate and grasp them in an automated way. Despite the advances in mobile manipulation technology, nowadays underwater operations are performed with a very low level of automation. State of the art ROVs are tele-operated and the robot arm control is performed in the counter-intuitive joint-space. Recently, some researchers, like Ridao et al. (2014), started to improve the automation level for underwater mobile manipulator operations introducing the concept of intervention autonomous underwater vehicles (I-AUVs).

The problem of navigating in an environment while mapping it at object level has been the subject of recent studies in mobile robotics (Salas-Moreno et al. (2013), Bowman et al. (2017), Dos Santos et al. (2017)). These methods use 3D object recognition, based on detecting the presence and location of objects whose model is known *a priori*. For the best of the authors known there are no similar studies in the underwater domain.

SLAM based navigation problem, has also caught attention of the underwater research community. Several solutions have been presented in the literature, to solve localization and mapping in the underwater domain using an AUV Ribas et al. (2007), Chen et al. (2013), Yuan et al. (2017). Our goal consists of using an automatic method for the recognition and location of 3D objects based on colourless 3D point clouds extracted from a laser scanner, and the integration of these measurements into an extended Kalman filter (EKF) simultaneous localization and mapping (SLAM) algorithm. Two main modules are necessary to achieve this goal: a 3D object recognition pipeline, responsible for recognizing and locating the objects present in the scene, and a real-time EKF-based

10.1016/j.ifacol.2018.09.497

semantic SLAM algorithm that uses the outcome of the first module to map the environment while avoiding AUV drift. A global feature descriptor is used to characterize the object scans. The purpose of using descriptors is to make the procedure of recognition much easier, where in order to compare two objects, we compare their descriptors.

The paper is organized as follows. Details of the proposed method as well as an introduction to 3D global descriptors are available in next section. Section III reports the experimental evaluation, showing results obtained with the Girona 500 AUV mounting an underwater laser scanner inside a water tank. The paper finalizes with a summary of conclusions as well as future work ideas.

2. METHODOLOGY

The two main components of our proposal are described next: the 3D object recognition pipeline and the feature-based semantic SLAM.

2.1 3D Object recognition pipeline

The block diagram of the proposed pipeline is shown in Fig. 1. The method uses, as an input, a 3D point cloud of the scene acquired with a laser scanner. The scene may include objects for which a 3D model is available *a priori* in a database. The goal of the algorithm is to identify these objects in the point cloud, as well as to locate them in the scanner frame. To bring this 3D object recognition technology underwater, two problems have to be addressed. First, it is necessary to use a real-time scanner able to provide dense 3D point clouds in real-time at a sufficient frequency (3 to 10 Hz). Second, it is required to adapt the object recognition and location methods reported in the literature to the complexities of the underwater environment. The modules integrating the pipeline are briefly described in the following subsections.

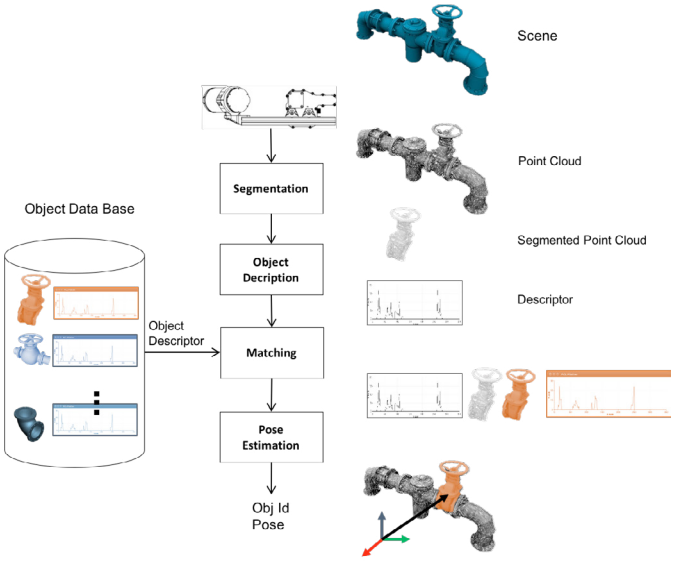

Fig. 1. Block diagram of the proposed pipeline.

Data gathering using an underwater laser scanner Land and aerial robots can use depth cameras for 3D perception and, in some cases, also RGB color information for each 3D point. Most of these sensors use infrared light, which attenuates very fast underwater. As such, they can only be used at very short ranges (i.e. 20 cm, see Digumarti et al. (2016)). Stereo cameras use visible light, which penetrates deeper than infrared light (depending on the wavelength) into the water. However, they rely on the presence of texture-based features to compute the 3D points, which normally implies the use of strong artificial illumination and the presence of natural texture in the environment. By contrast, laser scanners have the advantage that coherent laser light penetrates further than non-coherent light used for stereo cameras. Instead of RGB color information, laser scanners can sense the surface reflectance at the frequency of the laser illumination. Most of the commercially available laser scanners have an acquisition time which does not allow real-time operation. For this reason, our team designed and developed a (patent pending) real-time laser scanner which better fits the needs of this project (see Palomer et al. (2018)). This laser scanner consists of a laser line projector, a mirror steered with a galvanometer which projects the line at different parts of the scene through a flat viewport, and a camera with its own flat viewport. The control of the sensor, together with the laser detection implemented internally by the camera hardware, allows the sensor to work at higher acquisition rates than commercially available laser scanners. Moreover, the sensor uses the results of Palomer et al. (2017) to increase the 3D triangulation speed by using an elliptical cone to represent the light projected underwater, as the laser line is distorted because of the refraction of the flat viewport.

The laser scanner has been mounted on Girona 500 AUV Ribas et al. (2012) as shown in Fig. 2. Using fixed artificial landmarks, the position of the laser camera with respect to the robot body frame have been estimated.

Segmentation In order to be able to apply 3D descriptors, we need to separate the objects to be recognized from the rest of the scene. This step referred to as the segmentation of point clouds, is a fundamental step in our 3D recognition pipeline. The idea behind it, consist of clustering the points that represents the query object in one homogeneous cluster based on similar characteristics. The segmentation phase is split into two steps, following the method proposed in Rusu et al. (2009). Firstly, the plane that best fits the environment is estimated using the randomized M-estimator sample consensus (RMSAC). This steps assumes that the objects that we are trying to locate are displaced on a locally flat area. Secondly, the points in the 3D scan that belong to the plane are identified and removed. The remaining points are clustered using the Euclidean cluster extraction.

3D Global descriptors After the segmentation is completed, the following step consists of calculating a global descriptor for each segmented object. These descriptors encode shape or geometry information in a very compact way, thus facilitating object recognition. Following Guo et al. (2013), 3D object recognition methods can be divided into two groups: local methods based on local descriptors and global methods based on global descriptors. While

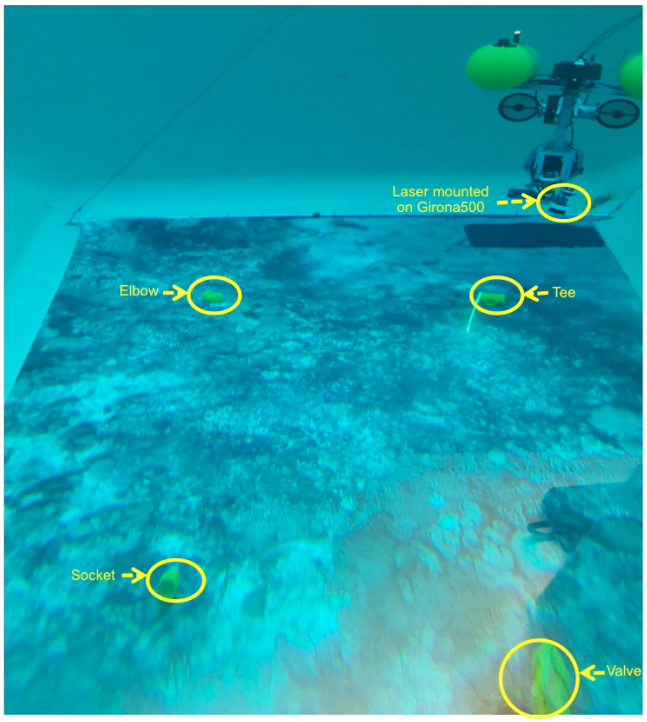

Fig. 2. Girona 500 AUV with the laser scanner mounted on it

.

the first category is more robust for environments with high object cluttering and occlusions, the second has a considerable lower computational cost which can facilitate real-time processing. For this reason global methods were chosen for the results of this paper.

For the experiments in this paper we have used Viewpoint Feature Histogram (VFH)(Rusu et al. (2010)) and the Ensemble of Shape Functions (ESF)(Wohlkinger and Vincze (2011)) descriptors. This choice was based on their state of the art performance in indoor environments (Rusu et al. (2010)).

Most of the 3D descriptors methods available in the PCL library compute normals as an internal step to characterize and represent features. Taking into account that most of the time we are dealing with noisy point clouds, the calculation of normals is not trivial. To account for this problem we also use the ESF descriptor, which is a normal-free method.

Matching The goal of the matching step is to identify a newly scanned object. This is done by comparing the global descriptor of the newly acquired object against descriptors of objects that have been scanned previously. Such objects form a database of objects that are recognizable.

Our database integrates four objects: a reducing tee, elbow, a reducing socket and ball valve. Each object is represented by a set of partial views. The acquisition of these views was performed offline and using a Microsoft Kinect sensor.

2.1.4.1. Matching based on Chi-square distance After computing the global descriptors, we compute and sort the distance between the new scanned object, and the object views included in the database, using the Chi-square distance as proposed in Rusu et al. (2008b) Hetzel et al. (2001). The smallest distance is used as the criterion to identify the newly scanned object among those in the database.

2.1.4.2. Matching based on Support Vector Machines In order to verify our histograms were behaving properly, we used a classification algorithm based on Support Vector Machines(SVM) (Boser et al. (1992)). Many studies have proven the superiority of SVM for classification compared to conventional methods. The SVM has increased generalization power and is robust even with highly-dimensional data, which allow to be used to learn nonlinear classification with the kernel function.

For classification we proceed as following:

- The four classes were enrolled to be classified. We used SVM multi-class implementation available in the OpenCV (Bradski (2000)) which is based on libsvm (Chang and Lin (2011)). The optimal parameter were performed from the paper Hsu et al. (2003), with radial basic function (RBF) kernel. For each class, the two descriptors were entered (ESF and VFH), meaning that the SVM classifier will classify the four groups (reducing tee, elbow, ball valve and reducing socket) only based on the descriptors, without taking into account the whole point cloud.
- To assess the performance of the SVM classifier we applied Leave One Out (LOO) cross-validation, since we have a small database. This method allows to test the test set independently from the training set. In LOO cross-validation, the data set (consisting of (N) features) is partitioned into complementary subsets: the training set (of size $(N-1)$) and the testing set comprising just one sample. This process is repeated N times, so that all samples are tried in turn.

The following table 1 and table 2 report the confusion matrix for the four classes using ESF features and VFH features respectively, based on SVM classifier. The rows correspond to actual classes, and the columns correspond to the classified ones to be assessed. The cells of the table show the possible correlations between the actual class and the predicted, where the diagonal cells marked in yellow correspond to the correctly identified class.

The result showed that the accuracy of SVM algorithm based on VFH features is low in comparison to ESF features. The classifier performs especially poor for the Elbow class, that was wrongly predicted as the Reducing Tee and Reducing Socket classes.

Pose Estimation After identifying the object, the iterative closest point (ICP) algorithm Besl and McKay (1992) is used to align the input scan with the scan of the matched object in the database. The output of the ICP is the relative pose of the object with respect to the laser scanner.

Table 1. Confusion matrix based ESF features for the four classes. yielding to 93.75% correct classification

Class	R_Tee	Elbow	Ball_Valve	R_Socket
R_Tee	7	0	1	0
Elbow	0	8	0	0
Ball_Valve	0	1	7	0
R_Socket	0	0	0	8

Table 2. Confusion matrix based VFH features for the four classes. yielding to 78.125% correct classification

Class	R_Tee	Elbow	Ball_Valve	R_Socket
R_Tee	8	0	0	0
Elbow	2	1	0	5
Ball_Valve	0	0	8	0
R_Socket	0	0	0	8

2.2 Simultaneous Localization And Mapping (SLAM)

SLAM deals with the problem of building a map of an unknown environment and using it to localize the vehicle simultaneously (see Smith et al. (1990) and Leonard and Durrant-Whyte (1991) for typical SLAM applications underwater).

The navigation filter implemented in the Girona 500 AUV is based on the EKF. It combines the navigation data gathered by a pressure sensor, a Doppler velocity log (DVL) and the attitude measured by an attitude and heading reference system (AHRS) to provide a dead-reckoning navigation. This navigation drifts over time and needs absolute measurements to correct it. Those measurements can come from either a global positioning system (GPS) when the vehicle is at the surface, or through the detection of visual landmarks in a map.

A semantic EKF-based SLAM filter is proposed here where landmark measurements are given by the 3D object recognition pipeline. The state vector for the implemented filter is the following:

$$\boldsymbol{x} = [x\ y\ z\ u\ v\ w\ l_1\ \dots\ l_N]\,, \tag{1}$$

where $[x\ y\ z]$ and $[u\ v\ w]$ are the position and linear velocity vectors of the AUV, and l_i is the landmark i pose vector defined as:

$$l_i = [lx_i\ ly_i\ lz_i\ l\phi_i\ l\theta_i\ l\psi_i]\,. \tag{2}$$

The navigation filter uses a constant velocity model with attitude input:

$$\hat{\boldsymbol{x}}_k = \begin{bmatrix} \begin{bmatrix} x_{k-1} \\ y_{k-1} \\ z_{k-1} \end{bmatrix} + \mathcal{R}(\phi_k\theta_k\psi_k) \left(\begin{bmatrix} u_{k-1} \\ v_{k-1} \\ w_{k-1} \end{bmatrix} t + \begin{bmatrix} n_{u_{k-1}} \\ n_{v_{k-1}} \\ n_{w_{k-1}} \end{bmatrix} \frac{t^2}{2} \right) \\ u_{k-1} + n_{u_{k-1}} \\ v_{k-1} + n_{v_{k-1}} \\ w_{k-1} + n_{w_{k-1}} \\ l_{1_{k-1}} \\ \dots \\ l_{N_{k-1}} \end{bmatrix}, \tag{3}$$

where t is the sample time, $[n_u\ n_v\ n_w]$ is the noise vector and $[\phi_k\ \theta_k\ \psi_k]$ are the Euler angles used as the filter input u_k.

Object detection measurements, are integrated in the filter as linear updates being

$$z_k = [lx_i\ ly_i\ lz_i\ l\phi_i\ l\theta_i\ l\psi_i], \tag{4}$$

and

$$H = \begin{bmatrix} -\mathcal{R}(\phi_k\theta_k\psi_k)^T & 0_{3\times3} & \mathcal{R}(\phi_k\theta_k\psi_k)^T & 0_{3\times3} & \dots \\ 0_{3\times3} & 0_{3\times3} & 0_{3\times3} & I_{3\times3} & \dots \end{bmatrix}, \tag{5}$$

where $[lx_i\ ly_i\ lz_i]$ is the relative position of the landmark with respect to the vehicle, $[\ l\phi_i\ l\theta_i\ l\psi_i]$ is the landmark orientation with respect the inertial frame, and $\mathcal{R}(\phi_k\theta_k\psi_k)$ is the vehicle orientation rotation matrix at time k.

3. EXPERIMENTAL RESULTS

In order to validate our approach, an experiment was performed in a water tank. A reducing tee object of $107 \times 74 \times 63\ mm^3$ was laid on the bottom of the tank, together with a reducing socket of $57 \times 43\ \times 63\ mm^3$, an elbow of $76 \times 41 \times 63\ mm^3$ and ball valve of $85 \times 125 \times 63\ mm^3$. The object database used for this experiment included all these four object models.

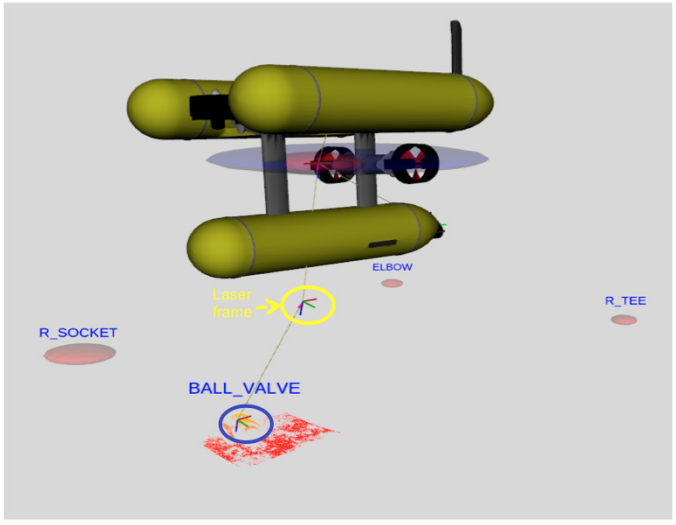

Fig. 3. Example of the recognition of the four objects using the ESF descriptor.

The GIRONA500 robot was teleoperated to follow an approximated square trajectory over these 4 objects that started from a position where the reducing socket was within the field of view of the laser scanner, continues to the elbow, then to the reducing tee, and finalizes in the ball valve. Approximately 3 complete loops were performed.

Objects were detected and identified using the proposed object recognition pipeline and its estimated position was used to update the state vector within the EKF-SLAM filter.

For each new measurement, the Mahalanobis distance, see Montiel and Montano (1998), with respect to the landmark, identified as the same object, was computed. If this distance was below a threshold, then the measurement was associated to it. If the measurement was not associated to any landmark already present in the filter, a new landmark was created if the measurement was observed consistently several times.

Fig. 4 shows the dead reckoning trajectory of the AUV as a blue line. The robot drifted along the trajectory mainly because it flew over the slopes of the water tank, which is known to generate a significant noise on the DVL readings (the purple ellipse shows its uncertainty). The EKF-SLAM corrected the drift of the AUV pose estimate as it can be appreciated in the trajectory represented by the red line in the same figure.

An image registration approach was used to generate ground-truth, as illustrated in Fig. 5. During the test, a standard optical camera acquired images of a known texture, laying at the bottom of the test pool. The position of the robot was estimated from point matches, with an accuracy of a few centimeters (Gracias and Santos-Victor (2001)).

Fig. 6, represents the covariance matrix plotted in two dimensions the abscise represents time-stamps and ordinate *the position of the robot* $\pm$ 3 $\times$ *sigma confidence bounds* with respect to the robot position. It is shown that every time that a landmark was detected (showed by green vertical lines), the uncertainty in the vehicle position was reduced.

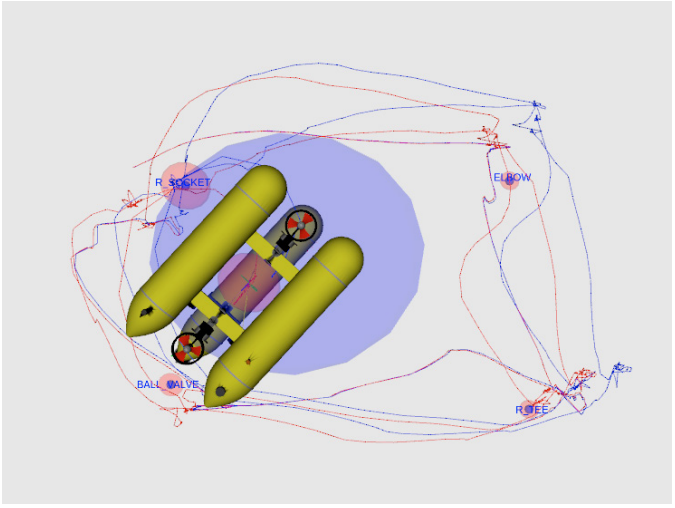

Fig. 4. Dead reckoning Trajectory in blue, trajectory corrected with the EKF-SLAM in red. The ellipsoids represent the 3 $\times$ *sigma confidence bounds*.

4. CONCLUSION

In this paper we have implemented a real-time localization and mapping system which exploits a 3D object recognition pipeline that allows to build maps at object level. Based on the experiments performed in a test tank, the results have shown that the 3D object recognition pipeline, based on the ESF and VFH global descriptors, was capable to recognize the scanned object among a set of objects, in the database. The ability to recognize 3D objects in real-time was also illustrated as a way to improve map accuracy when closing trajectory loops during SLAM.

ACKNOWLEDGEMENTS

This work was supported by the Spanish Government through a FPI Ph.D.grant to K. Himri and Project TWINBOT - Twin robots for underwater Intervention Missions (DPI2017-86372-C3-2R). Subproject: GIRONA 1000 - Cooperative Underwater Robot For Intervention.

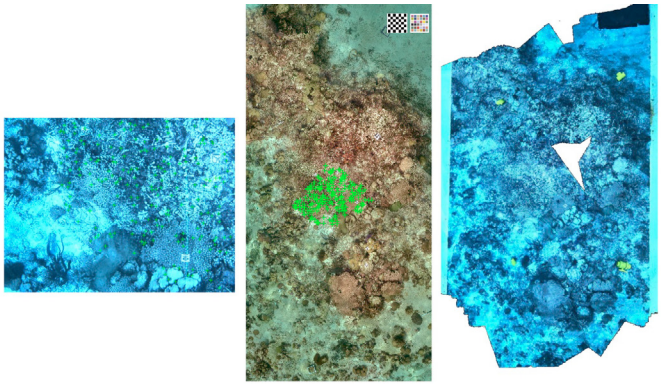

Fig. 5. Ground-truth creation using image registration. Original image acquired during the test (left), registration of this image against an image of the poster laying at the bottom of the test pool (center), and mosaic obtained from merging all images used for ground-truth (right).

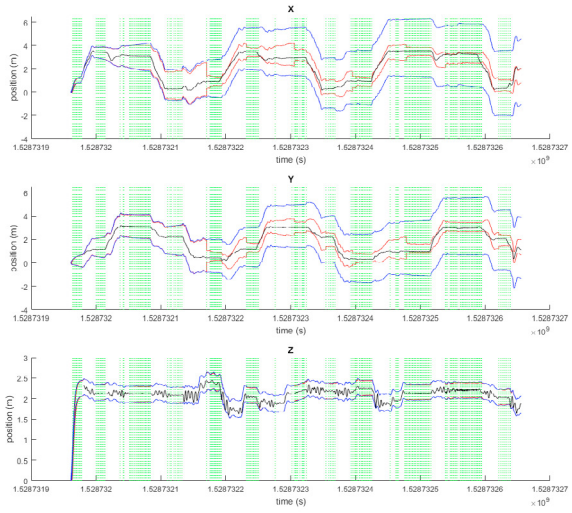

Fig. 6. The evolution of the covariance matrix in the three robot position (X, Y, Z). The dead-reckoning trajectory is marked in blue, the EKF-SLAM in red and the ground-truth in black.

REFERENCES

Besl, P.J. and McKay, N.D. (1992). Method for registration of 3-d shapes. In *Robotics-DL tentative*, 586–606. International Society for Optics and Photonics.

Blodow, N., Goron, L.C., Marton, Z.C., Pangercic, D., Rühr, T., Tenorth, M., and Beetz, M. (2011). Autonomous semantic mapping for robots performing everyday manipulation tasks in kitchen environments. In *Intelligent Robots and Systems (IROS), 2011 IEEE/RSJ International Conference on*, 4263–4270. IEEE.

Boser, B.E., Guyon, I.M., and Vapnik, V.N. (1992). A training algorithm for optimal margin classifiers. In *Pro-*

ceedings of the fifth annual workshop on Computational learning theory, 144–152. ACM.

Bowman, S.L., Atanasov, N., Daniilidis, K., and Pappas, G.J. (2017). Probabilistic data association for semantic slam. In *Robotics and Automation (ICRA), 2017 IEEE International Conference on*, 1722–1729. IEEE.

Bradski, G. (2000). The OpenCV Library. *Dr. Dobb's Journal of Software Tools*.

Chang, C.C. and Lin, C.J. (2011). Libsvm: a library for support vector machines. *ACM transactions on intelligent systems and technology (TIST)*, 2(3), 27.

Chen, L., Wang, S., McDonald-Maier, K., and Hu, H. (2013). Towards autonomous localization and mapping of auvs: a survey. *International Journal of Intelligent Unmanned Systems*, 1(2), 97–120.

Digumarti, S.T., Chaurasia, G., Taneja, A., Siegwart, R., Thomas, A., and Beardsley, P. (2016). Underwater 3D capture using a low-cost commercial depth camera. In *2016 IEEE Winter Conference on Applications of Computer Vision, WACV 2016*, volume 1. doi: 10.1109/WACV.2016.7477644.

Dos Santos, M., Ribeiro, P.O., Núñez, P., Drews-Jr, P., and Botelho, S. (2017). Object classification in semi structured enviroment using forward-looking sonar. *Sensors*, 17(10), 2235.

Gracias, N. and Santos-Victor, J. (2001). Trajectory reconstruction with uncertainty estimation using mosaic registration. *Robotics and Autonomous Systems*, 35, 163–177.

Guo, Y., Sohel, F., Bennamoun, M., Lu, M., and Wan, J. (2013). Rotational projection statistics for 3d local surface description and object recognition. *International journal of computer vision*, 105(1), 63–86.

Hetzel, G., Leibe, B., Levi, P., and Schiele, B. (2001). 3d object recognition from range images using local feature histograms. In *Computer Vision and Pattern Recognition, 2001. CVPR 2001. Proceedings of the 2001 IEEE Computer Society Conference on*, volume 2, II–II. IEEE.

Hsu, C.W., Chang, C.C., Lin, C.J., et al. (2003). A practical guide to support vector classification.

Leonard, J.J. and Durrant-Whyte, H.F. (1991). Mobile robot localization by tracking geometric beacons. *IEEE Transactions on robotics and Automation*, 7(3), 376–382.

Montiel, J. and Montano, L. (1998). Efficient validation of matching hypotheses using mahalanobis distance. *Engineering Applications of Artificial Intelligence*, 11(3), 439–448.

Palomer, A., Ridao, P., Forest, J., and Ribas, D. (2018). Underwater Laser Scanner: Ray-based Model and Calibration. *Manuscript submitted for publication*, 1–11.

Palomer, A., Ridao, P., Ribas, D., and Forest, J. (2017). Underwater 3D laser scanners: The deformation of the plane. In T.I. Fossen, K.Y. Pettersen, and H. Nijmeijer (eds.), *Lecture Notes in Control and Information Sciences*, volume 474, 73–88. Springer. doi:10.1007/978-3-319-55372-6_4.

Ribas, D., Palomeras, N., Ridao, P., Carreras, M., and Mallios, A. (2012). Girona 500 AUV: From survey to intervention. *IEEE/ASME Transactions on Mechatronics*, 17(1), 46–53.

Ribas, D., Ridao, P., Tardós, J.D., and Neira, J. (2007). Underwater slam in a marina environment. In *IEEE/RSJ International Conference on Intelligent Robots and Systems: 2007: IROS 2007, 2007, p. 1455-1460*. IEEE.

Ridao, P., Carreras, M., Ribas, D., Sanz, P.J., and Oliver, G. (2014). Intervention auvs: the next challenge. *IFAC Proceedings Volumes*, 47(3), 12146–12159.

Rusu, R.B., Blodow, N., Marton, Z.C., and Beetz, M. (2009). Close-range scene segmentation and reconstruction of 3d point cloud maps for mobile manipulation in domestic environments. In *Intelligent Robots and Systems, 2009. IROS 2009. IEEE/RSJ International Conference on*, 1–6. IEEE.

Rusu, R.B., Bradski, G., Thibaux, R., and Hsu, J. (2010). Fast 3d recognition and pose using the viewpoint feature histogram. In *Intelligent Robots and Systems (IROS), 2010 IEEE/RSJ International Conference on*, 2155–2162. IEEE.

Rusu, R.B., Gerkey, B., and Beetz, M. (2008a). Robots in the kitchen: Exploiting ubiquitous sensing and actuation. *Robotics and Autonomous Systems*, 56(10), 844–856.

Rusu, R.B., Marton, Z.C., Blodow, N., and Beetz, M. (2008b). Persistent point feature histograms for 3d point clouds. In *Proc 10th Int Conf Intel Autonomous Syst (IAS-10), Baden-Baden, Germany*, 119–128.

Rusu, R.B., Marton, Z.C., Blodow, N., Dolha, M., and Beetz, M. (2008c). Towards 3d point cloud based object maps for household environments. *Robotics and Autonomous Systems*, 56(11), 927–941.

Salas-Moreno, R.F., Newcombe, R.A., Strasdat, H., Kelly, P.H., and Davison, A.J. (2013). Slam++: Simultaneous localisation and mapping at the level of objects. In *Computer Vision and Pattern Recognition (CVPR), 2013 IEEE Conference on*, 1352–1359. IEEE.

Smith, R., Self, M., and Cheeseman, P. (1990). Estimating uncertain spatial relationships in robotics. In *Autonomous robot vehicles*, 167–193. Springer.

Wohlkinger, W. and Vincze, M. (2011). Ensemble of shape functions for 3d object classification. In *Robotics and Biomimetics (ROBIO), 2011 IEEE International Conference on*, 2987–2992. IEEE.

Yuan, X., Martínez-Ortega, J.F., Fernández, J.A.S., and Eckert, M. (2017). AEKF-SLAM: a new algorithm for robotic underwater navigation. *Sensors*, 17(5), 1174.